参赛学生姓名: 白双源
中学: 西安高新第一中学
省份: <u>陕西省</u>
国家/地区: 中国
指导老师姓名: <u>彭勤科</u>
指导老师单位: <u>西安交通大学</u>
企文题目: <u>不确定光照下的最优光伏电力</u>
定价机制研究:基于可靠性分级市场
(Research on the Optimal
Photovoltaic Power Pricing Mechanism
nder Uncertain Lighting: Based on
the Reliability Graded Market)

Research on the Optimal Photovoltaic Power Pricing Mechanism under Uncertain Lighting: Based on the Reliability Graded Market

Shuangyuan Bai, Xi'an Gaoxin No. 1 High School, Shaanxi Province, China Qinke Peng, Xi'an Jiaotong University, Shaanxi Province, China

Abstract

To reduce the reserve and frequency-regulation costs triggered by high-penetration photovoltaics, this paper proposes a variable reliability market design framework that does not rely on high accuracy forecasting. First, minute resolution output series are used to construct an availability curve, and a discrete ramping cost metric is introduced with units commensurate with capacity pricing. The availability curve separates daylight from nighttime segments and highlights the operational contrast between clear sky and cloudy regimes at medium to high output levels. The ramping metric compresses short run volatility into a settlement ready, auditable quantity that is dimensionally unified with capacity terms, allowing variability charges to be added to, or translated into, capacity based charges without altering existing market products or settlement plumbing. On this measurement foundation, we formulate three integration cost models (full information, partial information, and no information) and derive closed form indicators for grid integration cost and a subsidy rate that captures the extent to which variability costs are socialized. The models make transparent how incremental improvements in forecast quality map into reduced balancing needs and clearer price signals for producers and consumers.

In the broader policy context of decarbonization and the renewable buildout, the contract layer we advocate, which brings variability forward and prices it with dimensionally unified minute scale metrics, fits squarely within the mainstream framing of the green transition. Consistent with the UNEP's widely cited formulation, a green economy is one that improves human well being and social equity while significantly reducing environmental risks and ecological scarcities, typically characterized as low carbon, resource efficient and socially inclusive. By making variability explicit and priced with dimensionally unified minute scale metrics, our variable reliability design provides a settlement ready and auditable pathway that is aligned with the green economy transition.

Building on these measurements and cost characterizations, we design a variable reliability family of tiered capacity and pricing contracts, implemented through a transparent priority rule that guarantees feasibility in every realized state: total served load never exceeds realized PV output, and scarcity is resolved through orderly curtailment consistent with the contracted reliability tier. Prices can be supported either by shadow value interpretations or by cost based markups, making the mechanism auditable and compatible with prevailing energy and ancillary service arrangements while keeping ex ante terms and ex post verification straightforward. The contract layer therefore internalizes stochastic risk before real time and lets consumers voluntarily choose reliability and price bundles, aligning incentives without indiscriminate expansion of system side reserves.

We assess the framework using representative minute scale day profiles from two meteorologically distinct regions: Lanzhou (clear sky, relatively stable) and Guangzhou (cloud driven and rampy). Guangzhou's more frequent minute scale ramps are associated with markedly higher integration costs and subsidy rates than in Lanzhou, validating the sensitivity of the approach to regional heterogeneity and showing that exposing variability at the contract layer reduces rigid reserve requirements, lowers socialized costs, and improves the clarity and

ı

credibility of economic signals for both producers and consumers. Regional availability patterns naturally map into contract menus and markup factors, yielding a location aware design that respects local conditions without sacrificing market coherence.

On implementation, emphasis is placed on the discrete ramping cost metric. A threshold and event window are calibrated from local historical data using the sampling step and a canonical event duration; whenever a one step change exceeds the threshold, the entire step is counted under a whole step charging rule. With only a few tunable parameters, this construction turns high frequency fluctuations into a compact, noise tolerant, reproducible settlement variable that auditors can recompute directly from telemetry. Because it is dimensionally unified with capacity charges, the metric can be added to capacity payments or expressed as a capacity equivalent for benchmarking across regions and seasons, enabling phased pilots that scale as data quality and market familiarity grow. By revealing the price of balancing difficulty before real time, the design also strengthens interactions with storage and flexible loads, encouraging investment and improving utilization of existing assets.

Sensitivity analyses indicate that policy conclusions are robust to alternative event window definitions, threshold choices, and moderate data gaps; the ordering of contract options and the magnitude of regional cost differentials remain qualitatively unchanged. Limitations, such as possible nonstationarity under extreme weather regimes and the need for transparent governance when reliability menus evolve, are mitigated by periodic recalibration of availability profiles and ramp parameters and by publishing versioned inputs and audit trails. Overall, moving the price signal for balancing difficulty upstream into the contract layer, while centering a discrete, auditable, capacity commensurate ramping metric, offers a practical, scalable pathway to integrate large shares of PV without dependence on high accuracy forecasting, reduce socialized integration costs, and improve allocative efficiency across the system.

Index Terms

photovoltaics; minute-resolution variability; availability curve; discrete ramping-cost metric; dimensionally unified settlement; variable reliability; tiered capacity and pricing; integration costs

CONTENTS

I	Introduction						
II	Model	Modeling Photovoltaic Variability					
	II-A	Factors Affecting Photovoltaic Output	2				
	II-B	PV Availability Curve	4				
	II-C	Ramping-Cost Model	6				
	II-D	Dimensional Consistency	6				
Ш	Cost N	Models	7				
	III-A	Full-Information Forecast	7				
	III-B	No-Information Forecast	9				
	III-C	Partial-Information Forecast	9				
IV	Variab	ole-Reliability PV Market Design	11				
	IV-A	Mechanism and Contract Structure	11				
	IV-B	Utility and Social Welfare Maximization	12				
V	Case S	Studies and Regional Comparison	14				
	V-A	Parameter Settings and Output Modeling	14				
	V-B	Availability $G(x)$ Comparison	14				
	V-C	Ramping and Integration Cost Calculations	15				
	V-D	Contract Design	16				
VI	Conclu	asion	18				
Refe	rences		18				

I. Introduction

In recent years, the value of "reliability" has been explicitly priced and written into contracts, with differing approaches across jurisdictions. In California, for example, CAISO's *Resource Adequacy (RA)* framework requires load-serving entities to pre-arrange available capacity and introduces a *Flexible Ramping Product (FRP)* that effectively pays upfront to reserve upward and downward ramping capability to cover the uncertainty band of net load. On the regulatory side, the CPUC specifies which capacity must be procured locally versus system-wide and, in some cases, procures centrally—unbundling "adequacy" and "flexibility" and pricing them separately [1]–[4]. Intuitively, this is a "system-buys-first" path that makes volatility risk explicit through capacity and short-term flexibility products, with costs largely socialized on the demand side via compliance obligations.

By contrast, the EU emphasizes *long-term capacity contracts*. Under the Internal Market in Electricity Regulation (EU 2019/943), *capacity remuneration mechanisms* (*CRMs*) may be activated only when a supply shortfall is demonstrated, and they must be compatible with the energy market and allow cross-border participation [5], [6]. Many countries adopt *Reliability Options* (*ROs*): generators receive a capacity payment via centralized auctions and commit to availability during scarcity; when prices spike, they rebate revenues above the strike price—thus writing extreme-period price risk into the contract. Typical cases include Ireland's ISEM, which places ROs at the core of its CRM design, and Italy's Terna-run capacity market, which uses a one-sided CfD/RO-style structure with detailed performance rules [7]–[9]. In short, the EU path is to "sign long-term capacity contracts first and internalize scarcity risk in settlement."

China's "dual-carbon" targets and the 2030 renewable build-out plan have driven rapid PV and wind deployment under the twin engines of quota mandates and fiscal subsidies. However, the "non-dispatchable, intermittent, and variable" nature of renewables imposes new implicit costs on the grid: system operators must procure additional ramping and frequency-regulation reserves to maintain balance [10]–[13]. Assessments in some provinces indicate that as renewable penetration rises from 20% to above 30%, maximum upward reserve requirements can double, and minute-scale power fluctuations can reach 20% of nameplate capacity [14]. Such reserves are often provided by fast-start gas turbines, whose fuel use and emissions offset part of the green benefits [15]. If the "100% reliability" supply standard is retained, operators must maintain large quantities of reserve and frequency-control resources; the capital and operating costs grow nonlinearly and are indirectly embedded in tariffs as an implicit subsidy, becoming a key drag on market efficiency.

Here, "social subsidy" refers to the implicit support whereby the additional costs of reserves, grid reinforcement, and dispatch incurred by integrating intermittent renewables are shifted from project developers to all electricity consumers or to public finance. Social subsidy dilutes the technology's own uncertainty costs across all consumers, relieving generators from fully internalizing their variability. Its absolute value is denoted by CI, equal to grid-integration cost (see (14)), and its relative value by the subsidy rate σ (see (15)); together they measure the system-wide burden arising from variability. Framed in policy terms, the above "social subsidy" phenomenon is a classic externality problem of the energy transition. Academic and policy uses of the term "green economy" are broadly consistent: UNEP defines it as an economy that improves human well-being and social equity while reducing environmental risks and ecological scarcities, often summarized as low-carbon, resource-efficient and socially inclusive. Within this framing, our variable-reliability market design

1

operationalizes the green-economy agenda for high-PV systems by internalizing variability through minute-scale availability profiling and a discrete ramping-cost metric that is dimensionally unified with capacity charges, thereby converting externalities into contractible and auditable settlement items.

Early approaches to quantifying variability costs relied heavily on system simulations and reserve accounting [10]–[13]. In parallel, the electricity-economics literature proposed *reliability-differentiated pricing*, treating supply reliability as a tradable attribute so that consumers voluntarily assume part of the balancing obligation via menus; it further showed that if, at every node and time, the electricity price equals the marginal cost of one more unit of generation, the system endogenously minimizes total cost [16], [17]. Subsequent Priority Service / Demand Subscription frameworks bundle reliability for sale, enabling self-selection between price and reliability [18]–[20], and gave rise to instruments such as interruption insurance [21] and real-time pricing [22], [23], among others [24]–[26]. Recent work extends this logic to variable renewables by selling random energy or reliability-tiered contracts, thereby making variability costs explicit and internally settled [27], [28]. Nonetheless, three gaps remain: (i) most studies use hourly data and miss minute-scale ramps from cloud transients, causing a unit mismatch between capacity payments (/MW) and regulation charges ($/MW \cdot min$) [10], [11]; (ii) many models assume highly accurate forecasts or ample storage, underestimating integration costs under information frictions [12], [13]; and (iii) price–reliability coefficients are often set heuristically, lacking direct linkage to meteorological statistics, which limits engineering adoption [29].

Relative to these international practices, this paper takes a "contract-layer, minute-scale" route. Unlike California's system-level *advance procurement* of capacity and *flexible ramping* (RA/FRP) [1]–[4], and unlike the EU's approach of ensuring adequacy via long-term capacity contracts / ROs once a shortfall is identified [5]–[9], we price the "deliverability probability" directly in contracts: from minute-resolution PV series we construct an availability curve, and we propose an indicator-function aggregation formula for ramping charges that naturally converts $/MW \cdot min$ into capacity-commensurate /MW, placing variability cost on the same scale. We then derive closed-form expressions for integration cost and the subsidy rate under full-, partial-, and no-information scenarios to quantify the marginal value of forecast accuracy; and, using clear-sky Lanzhou and cloudy Guangzhou minute-series, we obtain closed-form capacity-price solutions that reveal how contract structures and cost allocations differ across meteorological regimes. In essence, we move the price signal of "balancing difficulty" upstream from the system level into buyer-seller contracts—complementing RA/FRP and CRM/RO without altering existing energy and ancillary-service frameworks—and show that this can materially reduce the social integration cost CI and subsidy rate σ . These results echo the predictions of responsive-pricing theory [18], [23], [24] and offer a practical market-based pathway for integrating high-penetration PV.

II. MODELING PHOTOVOLTAIC VARIABILITY

A. Factors Affecting Photovoltaic Output

Photovoltaic (PV) power output is significantly shaped by three classes of environmental drivers: (i) the diurnal cycle, (ii) synoptic weather conditions, and (iii) cloud motion.

(1) Diurnal Cycle: The diurnal cycle is the most fundamental periodic driver of PV output. Under ideal clear-sky conditions, PV power exhibits a single-peaked profile. A simple single-factor model can be written

as

$$X_{\text{day}}(i) = M \cdot \cos\left(\frac{\pi(i-12)}{I_{\text{day}}}\right), \quad i \in [6, 18],$$
 (1)

where I_{day} is the effective daylight duration (hours) and M is the plant nameplate capacity. The model implies a peak near local noon ($i \approx 12$) with output approaching zero at sunrise and sunset.

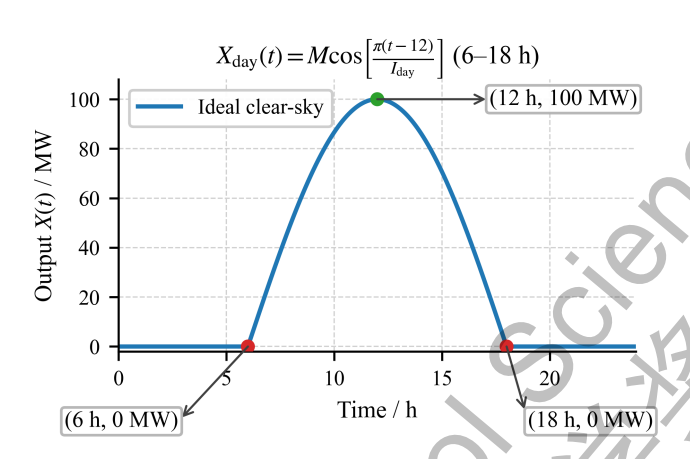


Fig. 1: Effect of the diurnal cycle on PV output.

As illustrated in Fig. 1, the horizontal axis is time (typically from 06:00 to 18:00), and the vertical axis is actual PV output in MW. With $M=100\,\mathrm{MW}$, the profile rises from near zero at sunrise, reaches its maximum around noon, and then declines toward zero by sunset. This baseline provides a reference for subsequent analysis under non-ideal conditions (e.g., clouds), where deviations from the single-peak curve can be attributed to additional weather-driven factors.

(2) Weather Conditions : Weather effects can be grouped into three typical regimes. In *clear-sky* conditions, irradiance is strong and stable, with energy yields at about 85%-100% of nameplate and minute-to-minute variability typically below 2% (e.g., $\leq 2\,\mathrm{MW}$ per minute when $M=100\,\mathrm{MW}$); the power trace is smooth. In *partly cloudy* conditions, intermittent shading lowers average output to roughly 50%-85% of nameplate and introduces flicker-like variations; minute-scale fluctuations can reach $\pm 10\%$, producing frequent ramp events. Under *overcast/rain* conditions, output may drop to 10%-30% of nameplate; variability is slower but the overall level remains persistently low.

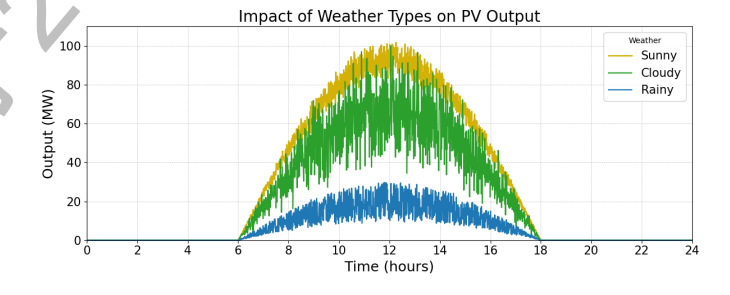


Fig. 2: PV output profiles under different weather regimes.

As shown in Fig. 2, the horizontal axis is time over a 24-hour day and the vertical axis is output. The clear-sky curve resembles the single-peaked baseline in Fig. 1; the partly cloudy curve exhibits reduced average output (about 50%-85% of nameplate) with pronounced jagged fluctuations; and the overcast/rain curve remains smooth but depressed (about 10%-30% of nameplate).

(3) Cloud Motion and Minute-Scale Ramps:

Cloud-shadow advection is a primary driver of PV variability. When cloud fields translate at $10 \,\mathrm{m\,s^{-1}}$ to $15 \,\mathrm{m\,s^{-1}}$, geographically proximate PV plants can fluctuate synchronously. The instantaneous ramp rate scales with cloud speed and the spatial gradient of irradiance:

$$\frac{\mathrm{d}X}{\mathrm{d}t} \propto \mathbf{v}_{\mathrm{cloud}} \cdot \nabla I_{\mathrm{solar}},$$
 (2)

where X is instantaneous PV output (power or a normalized index), $\mathbf{v}_{\text{cloud}}$ is the horizontal cloud-motion velocity (m s⁻¹), and ∇I_{solar} is the spatial gradient of irradiance (with I_{solar} in W m⁻², hence ∇I_{solar} in W m⁻³). The dot product captures how advection across irradiance inhomogeneity induces rapid changes in PV output.

This mechanism can produce $10\% \,\mathrm{min^{-1}}$ to $20\% \,\mathrm{min^{-1}}$ ramps. The sample below contrasts short-horizon fluctuations with and without pronounced cloud motion. As shown in Fig. 3,the horizontal axis is minutes and

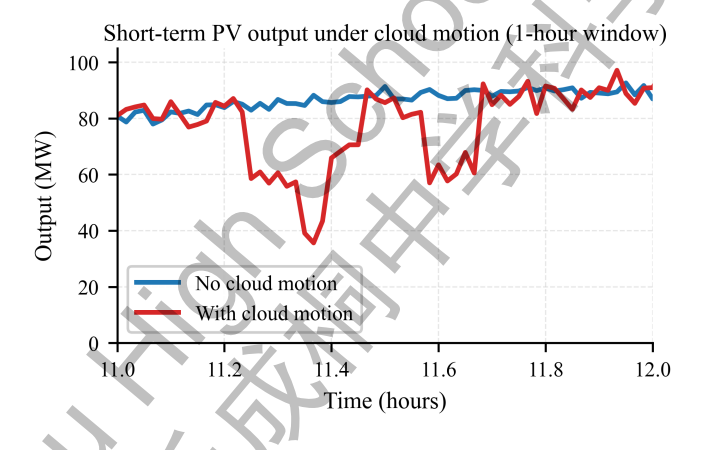


Fig. 3: Short-horizon PV fluctuations under cloud advection (zoomed view).

the vertical axis is output, highlighting minute-scale variabilityover a one-hour window at 1-min resolution the trace with cloud motion exhibits minute-scale dips and rebounds, whereas the baseline without cloud motion remains near 85 MW to 92 MW with only small minute-to-minute variation. In practice, ramping cost accounts for only a small share of total integration cost, yet it is non-negligible and should be made explicit in market design and settlement.

B. PV Availability Curve

The availability curve is defined by

$$G(x) = \max\left\{p: \frac{1}{n} \sum_{i=1}^{n} \mathbf{1}(X(i) \ge x) \ge p\right\},\tag{3}$$

where X(i) is realized output at time i and $\mathbf{1}(\cdot)$ is the indicator (1 if $X(i) \geq x$, 0 otherwise). Equivalently,

$$G(x) = \Pr(X_{\text{output}} > x), \tag{4}$$

i.e., the probability that output meets or exceeds threshold x.

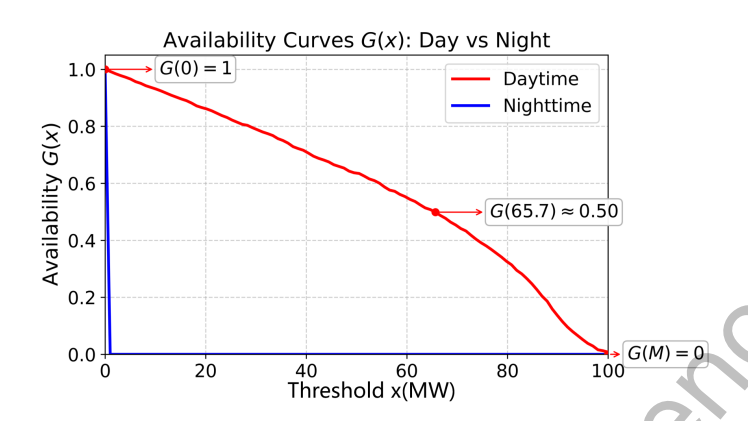


Fig. 4: Day vs. night availability G(x).

As shown in Fig. 4, the daytime availability curve starts at G(0)=1 and decays monotonically with the threshold x, whereas the nighttime curve collapses to $G(x)\approx 0$ for any x>0 (a jump at x=0), highlighting that PV alone cannot meet nocturnal demand. At night, $G(x)\approx 0$ for x>0 because $X(i)\approx 0$; during the day, G(x) decreases monotonically with x, quantifying the need for storage or backup to meet nocturnal demand.

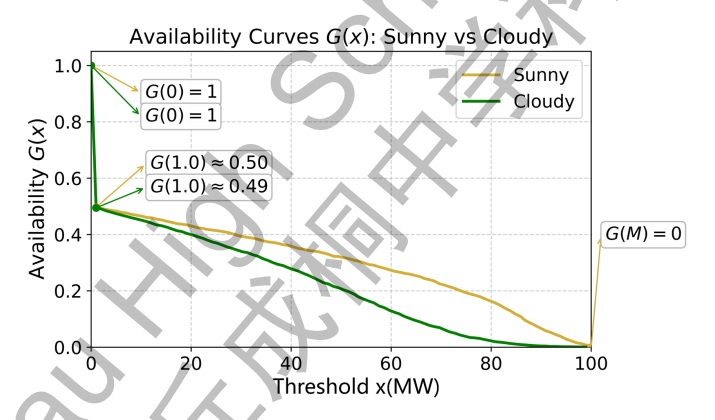


Fig. 5: Clear vs. cloudy availability G(x).

As shown in Fig. 5, both clear and cloudy cases satisfy G(0)=1. For small positive thresholds x>0, G(x) in both cases is close to 0.5, reflecting roughly 12 hours of daylight versus 12 hours of night. As x increases, G(x) declines monotonically; the clear-sky curve remains uniformly above the cloudy one and falls more slowly with x, indicating higher availability and lower intermittency at medium-high power levels (e.g., $x \gtrsim 60 \, \mathrm{MW}$).

C. Ramping-Cost Model

For a realized series $\{X_i\}_{i=1}^N$, define

$$C_{\text{ramp}} = c_r \sum_{i=1}^{N} \mathbf{1} (\Delta X_i > \Delta X_{\text{th}}) \, \Delta X_i, \tag{5}$$

$$\Delta X_i = |X_i - X_{i-1}|,\tag{6}$$

$$\Delta X_{\rm th} = \delta M \, \frac{\Delta t}{\Delta t_{\rm event}},\tag{7}$$

where c_r is the unit charge, M is nameplate capacity, Δt is the sampling interval (1 min), and $\Delta t_{\rm event}$ is a representative event duration (10 min). The threshold triggers charging but does not clip the step: whenever $\Delta X_i > \Delta X_{\rm th}$, the entire ΔX_i is charged at rate c_r . If Δt or $\Delta t_{\rm event}$ changes, only $\Delta X_{\rm th}$ needs rescaling; the form of (5) is unchanged.

D. Dimensional Consistency

We map minute-scale "steep-ramp" regulation difficulty onto the same scale as the capacity term so that ramping costs can be combined with the integration cost CI under commensurate units (measured against MW). Within a threshold-event-window framework, a "ramp rate" over a canonical event duration $\Delta t_{\rm event}$ is integrated into an *equivalent power increment*, so charges are assessed by magnitude rather than by rate. Let the sampling step be Δt , the nameplate/contract capacity be M, and the allowed ramp rate be δ (fraction of capacity per minute). Define

$$\Delta X_{
m th} = \delta \, M \cdot \frac{\Delta t}{\Delta t_{
m event}}, \qquad \Delta X_i = |X_i - X_{i-1}|,$$

and write the ramping cost per unit capacity as

$$\widetilde{C}_{\text{ramp}} = \frac{C_{\text{ramp}}}{M} = c_r \sum_{i=1}^{N} \mathbf{1}(\Delta X_i > \Delta X_{\text{th}}) \frac{\Delta X_i}{M}, \tag{8}$$

where c_r prices the magnitude of the step so that the units of c_r cancel those of $\Delta X_i/M$, making $\widetilde{C}_{\mathrm{ramp}}$ per MW. Here $\Delta t_{\mathrm{event}}$ (set to $10\,\mathrm{min}$) converts a rate into a quantity over the event window, and Δt (set to $1\,\mathrm{min}$) is the sampling interval. For an approximately monotone ramp lasting τ with average rate $r = \Delta X_i/\Delta t$ that satisfies $r > \delta M/\Delta t_{\mathrm{event}}$, the condition $\Delta X_i > \Delta X_{\mathrm{th}}$ holds for all steps within the event and $\sum \Delta X_i = r\tau = |X_{t_{\mathrm{end}}} - X_{t_{\mathrm{start}}}|$. The event cost is then $c_r \, r \, \tau = c_r \, |\Delta X_{\mathrm{event}}|$, showing insensitivity to the sampling granularity Δt and that integrating "rate" over $\Delta t_{\mathrm{event}}$ naturally yields a "quantity."

Define the capacity-equivalent

$$M_{\rm eq} = \frac{C_{\rm ramp}}{c},\tag{9}$$

which puts ramping on the same MW scale as the capacity price c (/MW). The integration cost can then be written as

$$CI(\alpha) = c \left[\frac{M}{2} (1 - H(\alpha)) + M_{\text{eq}} \right],$$
 (10)

where the first term is the capacity-equivalent cost induced by reliability layering (decreasing with the accuracy function $H(\alpha)$), and the second term is the capacity-equivalent consumption due to minute-scale ramps. The two terms share the same dimension and can be added directly for contract settlement or sensitivity analysis.

Compared with existing approaches, this dimensional reconciliation is essential. "Mileage/trajectory integral" methods charge all tracking motion via $\sum_i |\Delta X_i|$ or $\int |\dot{X}| \, dt$, typically settled at prices per MW·min; these units are not directly comparable to capacity price and the metric is sensitive to measurement noise and high-frequency jitter. "Ramp-rate penalties" of the form $\sum_i (|\Delta X_i|/\Delta t)$ still charge a rate and thus depend on time resolution and filtering choices. System-side flexible ramping products procure *capability* (MW) day-ahead/real-time, which concerns available capacity rather than realized event magnitudes.

By using a threshold–event-window construction, we move the physical condition "exceeding the dispatchable ramp rate" up to the contract layer and, once the threshold is crossed, charge by the *full magnitude* of the step rather than only the excess. This concentrates price signals on the minutes that actually pull reserves. The explicit $\Delta t_{\rm event}$ converts "rate" into an equivalent power increment so that c_r immediately yields monetary cost on the MW scale; through $M_{\rm eq}=C_{\rm ramp}/c$ it aligns seamlessly with the capacity term. The design remains numerically robust under changes of Δt or the event window by rescaling $\Delta X_{\rm th}$, and it naturally filters out fine-grained tracking and noise—offering advantages in unit consistency, comparability, and contractual implementability.

III. COST MODELS

To quantify PV integration costs and the associated subsidy needs, we develop three scenarios distinguished by the producer's forecast accuracy. For each scenario we compute the PV producer's profit, the additional cost required for grid integration (the social subsidy), and how these costs depend on information quality.

A. Full-Information Forecast

(1) Cost Formulation: Under full information, the producer can perfectly predict future output (e.g., knowing in advance the output at each hour of tomorrow). The producer sells \overline{M} MW of "100% firm" power at unit price c and procures just enough reserves to cover shortfalls. Let c_1 and c_2 denote the unit prices (per MW) of reserve capacity and reserve energy, respectively. In the full-information case, the producer procures $(\overline{M} - x)_+$ MW of reserves, where x is the realized output and $(z)_+ = \max\{z, 0\}$.

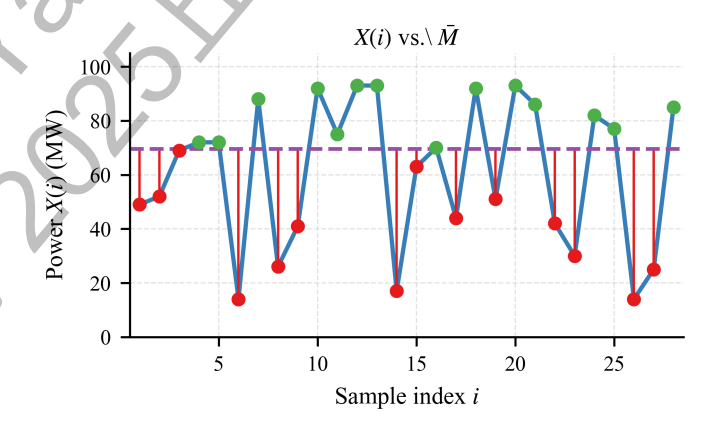


Fig. 6: Profit accounting under full information.

As shown in Fig. 6, a stylized realization X(i) is plotted against the contracted firm level \overline{M} (purple dashed line). Green markers indicate periods with surplus $(X(i) \geq \overline{M})$. Red markers and the vertical red segments

indicate shortfalls; the length of each segment is exactly $(\overline{M}-X(i))_+$, i.e., the reserve that must be procured in that minute. Summing these red segments over time approximates the discrete shortfall $\sum_i (\overline{M}-X(i))_+$, whose expectation equals the integral term in (11). Thus the figure makes clear that the second term in (11) is the expected cost of covering all shortfalls (capacity plus energy), while $c\overline{M}$ is the revenue and C_{ramp} accounts for minute-scale ramping cost (not drawn). Let $G(x) = \Pr(X \ge x)$ be the availability curve and F(x) = 1 - G(x) the cdf of output X. Write $-G_x \equiv -\frac{\mathrm{d}}{\mathrm{d}x}G(x) = F'(x)$ for the density. The expected profit is

$$\pi_{1} = \max_{\overline{M}} \left\{ c \, \overline{M} - (c_{1} + c_{2}) \int_{0}^{\overline{M}} (\overline{M} - x)_{+} (-G_{x}) \, \mathrm{d}x - C_{\mathrm{ramp}} \right\}, \tag{11}$$

where C_{ramp} is the total ramping cost defined earlier. The first-order condition with respect to \overline{M} yields

$$F(\overline{M}) = \frac{c}{c_1 + c_2}, \qquad F(x) = 1 - G(x).$$
 (12)

Assuming $X \sim \text{Unif}[0, M]$, we obtain

$$\overline{M} = \frac{c}{c_1 + c_2} M, \qquad \pi_1 = \frac{1}{2} \frac{c^2}{c_1 + c_2} M - C_{\text{ramp}}.$$
 (13)

(2) Numerical Illustration : We set $c_1=10/{\rm MW},\,c_2=60/{\rm MW},\,c=55/{\rm MW},\,{\rm and}\,\,c_r=0.80/{\rm MW}$ for a concrete calculation. From $\overline{M}=\frac{c}{c_1+c_2}M$ we obtain

$$\overline{M} = \frac{55}{10+60} M \approx 0.785 M.$$

If no reserves were required, the producer would simply sell all PV energy and earn the benchmark expected profit $\frac{1}{2}cM$.

For ramping costs, assume three effective ramp events per day. Each event has a magnitude $\Delta X_{\rm event} = 0.2M$, and every one-minute step within the event exceeds the threshold $\Delta X_{\rm th}$. With sampling $\Delta t = 1$ min and $\Delta t_{\rm event} = 10$ min, take $\Delta X_{\rm th} = 0.01M$. Then each event contributes 10 threshold-exceeding steps of size 0.02M, so

$$C_{\text{ramp}} = 0.8 \times 0.02M \times 3 \times 10 = 0.48M,$$

and the same ramp-cost assumption is adopted in subsequent calculations.

The grid-integration cost CI_1 and its normalized share σ_1 are

$$CI_1 = \frac{cM}{2} - \pi_1 = \frac{cM}{2} \left(1 - \frac{c}{c_1 + c_2} \right) + 0.48M,$$
 (14)

$$\sigma_1 = \frac{CI_1}{\frac{1}{2}cM} = 23.2\%. \tag{15}$$

Expression (14) shows that CI_1 has two components: (i) $\frac{cM}{2} \left[1 - \frac{c}{c_1 + c_2} \right]$, the expected cost of procuring reserve capacity and energy to ensure delivery of the firm commitment; and (ii) the added ramping cost 0.48M, which accounts for minute-scale variability drawing on system balancing resources. Normalizing by the nominal capacity term $\frac{1}{2}cM$ via (15) yields $\sigma_1 = 23.2\%$, indicating that, under these parameters, variability raises the social cost by nearly one quarter.

B. No-Information Forecast

(1) Cost Formulation: With no information, the producer cannot forecast beyond knowing the output distribution. To avoid default on the firm commitment, it must pre-procure reserve capacity equal to the committed level. Thus the producer sells \overline{M} MW at unit price c, purchases \overline{M} MW of reserve capacity at price c_1 , and, when realized output is x, buys real-time reserve energy $(\overline{M}-x)_+$ at price c_2 . The expected profit is

$$\pi_2 = \max_{\overline{M}} \left\{ c \, \overline{M} - c_1 \, \overline{M} - c_2 \int_0^{\overline{M}} (\overline{M} - x)_+ \, (-G_x) \, \mathrm{d}x - C_{\mathrm{ramp}} \right\},\tag{16}$$

where $G(x) = \Pr(X \ge x)$, F(x) = 1 - G(x), and $-G_x = \frac{\mathrm{d}}{\mathrm{d}x}F(x)$ is the density. The first-order condition gives

$$F(\overline{M}) = \frac{c - c_1}{c_2},$$

$$\overline{M} = \frac{c - c_1}{c_2} M.$$
(17)

$$\overline{M} = \frac{c - c_1}{c_2} M. \tag{18}$$

Under $X \sim \text{Unif}[0, M]$, the maximum profit is

$$\pi_2 = \frac{1}{2} \frac{(c - c_1)^2}{c_2} M - C_{\text{ramp}}.$$
(19)

(2) Numerical Illustration: Using $c_1 = 10/\text{MW}$, $c_2 = 60/\text{MW}$, c = 55/MW, and the same ramp-cost assumption $C_{\rm ramp} = 0.48\,M$ as before, we obtain

$$\overline{M} = \frac{c - c_1}{c_2} M = \frac{55 - 10}{60} M = 0.75 M.$$

The grid-integration cost and its normalized share are

$$CI_2 = \frac{cM}{2} \left[1 - \frac{(e - c_1)^2}{c c_2} \right] + 0.48 M,$$

$$\sigma_2 = \frac{CI_2}{\frac{1}{2}cM} = 40.4\%.$$
(20)

$$\sigma_2 = \frac{CI_2}{\frac{1}{2}eM} = 40.4\%. \tag{21}$$

Here CI_2 combines the expected cost of capacity and energy reserves implied by the no-information commitment with the minute-scale ramping cost; σ_2 expresses the total as a share of the nominal capacity term $\frac{1}{2}cM$.

C. Partial-Information Forecast

In practice, producers neither have perfect foresight nor face complete ignorance; partial information (e.g., from weather forecasts) is available. The producer chooses reserve purchases based on the committed firm quantity \overline{M} and the predicted output x_{pred} . Forecast errors cause either excess capacity (waste) or emergency purchases; we parameterize the resulting penalty by a deviation-cost coefficient γ . The profit maximization is

$$\pi_{3} = \max_{\overline{M}} \left\{ c \overline{M} - \left[c_{1} \mathbb{E}[(\overline{M} - x_{\text{pred}})_{+}] + c_{2} \mathbb{E}[(\overline{M} - x_{\text{real}})_{+}] + \gamma \mathbb{E}[|x_{\text{real}} - x_{\text{pred}}|] \right] - C_{\text{ramp}} \right\}, \tag{22}$$

where $\mathbb{E}[\cdot]$ denotes expectation, x_{pred} is the forecast, and x_{real} is the realized output. The first two expectations represent the capacity reserved ex ante (based on the forecast) and the shortfall energy needed ex post (based on the realization). The deviation term $\mathbb{E}[|x_{\text{real}} - x_{\text{pred}}|]$ captures the mismatch between purchased and required reserves. The ramping cost C_{ramp} does not depend on forecast accuracy and follows the earlier definition.

Because π_3 depends on forecast quality, a closed form in terms of a specific distribution for x_{pred} is not imposed. Instead, we interpolate between the full- and no-information benchmarks and model the grid-integration cost as

$$CI(\alpha) = \frac{cM}{2} \left[1 - H(\alpha) \right] + C_{\text{ramp}}, \tag{23}$$

where $\alpha \in [0,1]$ indexes forecast quality and $H(\alpha)$ is anchored at the two limits and interpolated by a concave power law:

$$H(\alpha) = H_0 + (H_1 - H_0) \alpha^{\beta}, \qquad 0 < \beta < 1,$$
 (24)

$$H_0 = \frac{(c - c_1)^2}{c c_2}, \qquad H_1 = \frac{c}{c_1 + c_2}.$$
 (25)

Hence,

$$CI(\alpha) = \frac{cM}{2} \left[1 - H_0 - (H_1 - H_0)\alpha^{\beta} \right] + C_{\text{ramp}}.$$
 (26)

Taking derivatives gives

$$\frac{\mathrm{d}CI}{\mathrm{d}\alpha} = -\frac{cM}{2} \left(H_1 - H_0 \right) \beta \,\alpha^{\beta - 1} < 0,\tag{27}$$

$$\frac{\mathrm{d}^{2}CI}{\mathrm{d}\alpha^{2}} = \frac{cM}{2} (H_{1} - H_{0}) \beta (1 - \beta) \alpha^{\beta - 2} > 0,$$
(28)

so $CI(\alpha)$ is decreasing in α with diminishing returns (steeper gains at low accuracy, flattening at high accuracy). Boundary values satisfy $CI(0) = \frac{cM}{2}[1-H_0] + C_{\mathrm{ramp}}$ and $CI(1) = \frac{cM}{2}[1-\frac{c}{c_1+c_2}] + C_{\mathrm{ramp}}$. To ensure $H(\alpha) \in [0,1]$ and monotonicity from H_0 to H_1 , take the feasible price domain $c \leq c_1 + c_2$ and $H_1 \geq H_0$, the latter equivalent to $c^2c_2 \geq (c_1+c_2)(c-c_1)^2$ (or $c_2 \geq \frac{(c-c_1)^2}{2c-c_1}$ when $2c > c_1$), together with $H_0 \leq 1$ (i.e., $c_2 \geq \frac{(c-c_1)^2}{c}$). Within this domain the semi-information results satisfy $\sigma_1 < \sigma_3 < \sigma_2$ and $CI_1 < CI_3 < CI_2$. The choice of the concave interpolant $1-\alpha^\beta$ reflects that marginal forecast improvements decline: in practice, low-cost signals (basic meteorology) yield large initial error reductions, whereas near 90% accuracy, additional data and modeling (satellite imagery, radar, deep learning) mainly contend with irreducible noise and yield smaller gains.

A visualization of overall profit under the semi-information model can be produced based on (23)–(26).

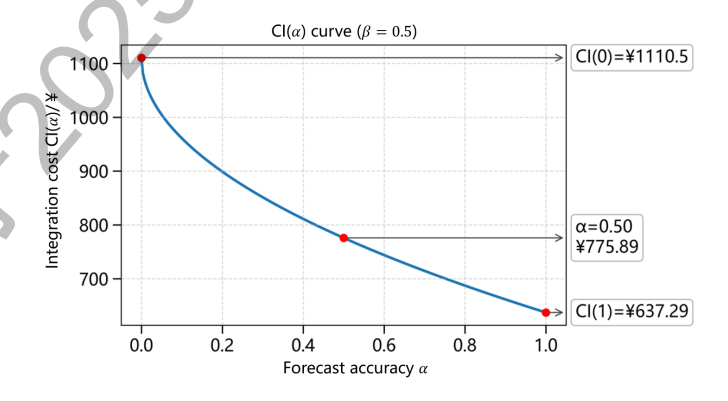


Fig. 7: Integration cost $CI(\alpha)$ vs. forecast accuracy α ($\beta = 0.5$).

As shown in Fig. 7, the horizontal axis is forecast accuracy α and the vertical axis is the grid-integration cost. At $\alpha = 0$ (no information), $CI \approx 1110.50$; at $\alpha = 1$ (full information), $CI \approx 637.20$. Both endpoints are consistent with (26) and the scenario definitions.

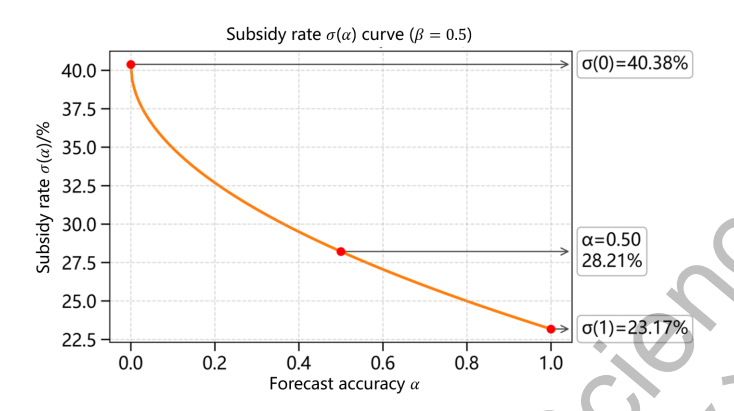


Fig. 8: Subsidy rate $\sigma(\alpha)$ vs. forecast accuracy α ($\beta = 0.5$)

Similarly, Fig. 8 shows the subsidy rate. The endpoint values at $\alpha = 0$ and $\alpha = 1$ correspond to the no-information and full-information cases, respectively (cf. σ_2 and σ_1 , computed earlier as 40.4% and 23.2%). Both visualizations use the concave power-law interpolation with $\beta = 0.5$ in (24).

IV. VARIABLE-RELIABILITY PV MARKET DESIGN

If stochastic PV energy is fully forced to be "firm," the required reserves rise sharply and costs escalate. To share uncertainty more efficiently, we design a market mechanism in which PV producers sell energy at differentiated reliability levels to consumers who voluntarily accept supply risk in exchange for lower prices. The key idea is that uncertainty is absorbed by the *contracts* rather than by system-side reserve procurement: PV output is presold in day-ahead tiers by delivery probability $\{\rho_k\}$, and a priority allocation rule $R_{\omega}(t)$ is fixed ex ante so that, for every realized state ω ,

$$\int_0^1 d(t) R_{\omega}(t) dt \le S(\omega), \tag{29}$$

where d(t) is the contracted quantity (MW) for consumer t, $R_{\omega}(t) \in \{0,1\}$ indicates service in state ω , and $S(\omega)$ is the realized PV supply (MW). Thus the total served load never exceeds realized output. When supply is insufficient, low-reliability contracts are curtailed according to the pre-specified order, without compensation; the shortfall is borne by the consumers who opted for lower ρ , rather than by system-wide reserves.

Prices make risk explicit: lower ρ carries a lower energy price, while higher ρ approaches the cost of firm supply. Because every random state is already partitioned by the contract structure, physical shortfalls are transformed into contractually acceptable curtailments, eliminating the need for additional socialized reserves to backstop PV stochasticity.

A. Mechanism and Contract Structure

In the day-ahead market, the producer offers a menu of reliability-differentiated contracts. Each tier is denoted (ρ_k, p_k) , where $\rho_k \in (0, 1]$ is the delivery probability and p_k is the corresponding price; higher ρ_k commands

a higher price. Consumers $t \in [0,1]$ choose a pair $(\rho(t), d(t))$, meaning they purchase d(t) at reliability $\rho(t)$. In real time, given realized PV $S(\omega)$, allocations follow a fixed priority rule in favor of higher reliability.

Formally, let $R_{\omega}(t) \in \{0, 1\}$ indicate whether consumer t is served in state ω . Feasibility and reliability are enforced by

$$\mathbb{P}(R_{\omega}(t) = 1) = \rho(t), \qquad \int_{0}^{1} d(t) R_{\omega}(t) dt \leq S(\omega), \tag{30}$$

i.e., the expected service probability matches the contracted reliability, and the total service in each state does not exceed realized supply. A monotone priority rule (higher ρ weakly dominates lower ρ in every state) implements these constraints while aligning prices with the accepted risk.

B. Utility and Social Welfare Maximization

Let U(d) denote a consumer's utility from receiving quantity d and L(d) the loss if curtailed. Assume U(0) = L(0) = 0 and U, L are increasing and convex. Because delivery is probabilistic, a contract (d, ρ) yields expected net utility

$$U_t(d,\rho) = \rho U(d) - (1-\rho)L(d).$$
 (31)

Aggregating over a continuum of consumers $t \in [0, 1]$, social welfare is

$$W = \int_0^1 \left[\rho(t) U(d(t)) - (1 - \rho(t)) L(d(t)) \right] dt, \tag{32}$$

to be maximized subject to the feasibility and reliability constraints in (30) under a discrete set of output states $\{s_1 < \dots < s_n\}$ with probabilities $\{\pi_1, \dots, \pi_n\}$, $\sum_{i=1}^n \pi_i = 1$.

We implement n contract tiers. Tier i offers reliability ρ_i with price p_i , ordered so that $\rho_1 > \rho_2 > \cdots > \rho_n$. Consumers $t \in [t_{i-1}, t_i)$ choose tier i and purchase d_i . In state s_i , only tiers with index $j \leq i$ (higher reliability) are served. Formally,

$$0 < s_1 < s_2 < \dots < s_n, \qquad \sum_{i=1}^n \pi_i = 1.$$
 (33)

Priority order is welfare-improving.: Consider two contracts $A(\rho_A, d_A)$ and $B(\rho_B, d_B)$ with $\rho_A > \rho_B$. For a small reallocation $\delta > 0$ of service, their marginal welfare gains are

$$\Delta W_A = \rho_A U'(d_A) \,\delta - (1 - \rho_A) L'(d_A) \,\delta, \tag{34}$$

$$\Delta W_B = \rho_B U'(d_B) \delta - (1 - \rho_B) L'(d_B) \delta. \tag{35}$$

Since U', L' > 0 and $\rho_A > \rho_B$, reallocating δ from B to A raises welfare. Repeating eliminates all "reverse-order" allocations and yields a monotone priority rule

$$R_{\omega}^{*}(t) = \begin{cases} 1, & t \in [0, t_{i}^{*}], \ S(\omega) = s_{i}, \\ 0, & \text{otherwise,} \end{cases}$$
 (36)

with induced reliabilities

$$\rho_i^* = \Pr[S(\omega) \ge s_i] = \sum_{i=1}^n \pi_j.$$
(37)

Cumulative feasibility implies

$$s_i = \sum_{j=1}^{i} d_j (t_j^* - t_{j-1}^*), \qquad s_{i-1} = \sum_{j=1}^{i-1} d_j (t_j^* - t_{j-1}^*),$$
 (38)

hence

$$s_i - s_{i-1} = d_i (t_i^* - t_{i-1}^*), (39)$$

which links the size of tier-i's customer set to its per-customer allocation. Therefore

$$d_i^* = \frac{s_i - s_{i-1}}{t_i^* - t_{i-1}^*}. (40)$$

Shadow pricing and individual optimality.: Introduce a shadow price $\mu \geq 0$ for the reliability-filtered resource. A representative consumer's Hamiltonian (surplus) is

$$H(d, \rho, \mu) = \rho U(d) - (1 - \rho) L(d) - \mu d.$$
(41)

An optimal contract (ρ^*, d^*) satisfies

$$H(d^*, \rho^*, \mu) = \max_{d, \rho} H(d, \rho, \mu) = H^*,$$
 (42)

together with feasibility and complementary slackness (market clearing). The first-order condition for d_i^* (given ρ_i and μ) is

$$\rho_i U'(d_i^*) - (1 - \rho_i) L'(d_i^*) = \mu, \tag{43}$$

i.e., marginal social benefit equals the marginal resource cost.

Tier-wise optimal contracts.: There exist $0 = t_0^* < t_1^* < \dots < t_k^* = 1$ with $k \le n$ such that for any $t \in [t_{i-1}^*, t_i^*)$,

$$d_i^* = \arg\max_{d} \left\{ \rho_i^* U(d) - (1 - \rho_i^*) L(d) - p_i^* d \right\}, \tag{44}$$

$$d_i^* = \frac{s_i - s_{i-1}}{t^* - t^*},\tag{45}$$

$$\rho_i^* = \sum_{j=i}^n \pi_j,\tag{46}$$

$$R_{\omega}^*(t) = \begin{cases} 1, & t \in [0, t_i^*], \ S(\omega) = s_i, \\ 0, & \text{otherwise.} \end{cases}$$

$$(47)$$

Given a target consumer surplus H^* , (44) and (45) jointly determine each tier's purchase d_i^* and the measure of consumers assigned to that tier, while satisfying the supply constraints and implementing reliability through the priority rule.

a) Producer revenue and welfare decomposition.: The producer's expected revenue is

$$\pi = \int_0^1 p(t) d(t) dt = \sum_{i=1}^n p_i \int_{t_{i-1}}^{t_i} d_i dt = \sum_{i=1}^n p_i d_i (t_i - t_{i-1}) = \sum_{i=1}^n p_i (s_i - s_{i-1}),$$
 (48)

where, under the optimal priority allocation, tier i serves consumers $t \in [t_{i-1}, t_i)$ with per-customer quantity $d_i = \frac{s_i - s_{i-1}}{t_i - t_{i-1}}$.

The producer's (gross) profit under the optimal allocation is therefore

$$\max \pi = \sum_{i=1}^{n} p_i (s_i - s_{i-1}). \tag{49}$$

Social welfare—producer surplus plus consumer surplus—equals

$$W^* = \sum_{i=1}^{n} (t_i^* - t_{i-1}^*) \left[\rho_i^* U(d_i^*) - (1 - \rho_i^*) L(d_i^*) \right]$$

$$= \sum_{i=1}^{n} (t_i^* - t_{i-1}^*) \left[p_i^* d_i^* + H_i^* \right]$$

$$= \sum_{i=1}^{n} p_i^* (s_i - s_{i-1}) + \sum_{i=1}^{n} (t_i^* - t_{i-1}^*) H_i^*,$$

$$= \sum_{i=1}^{n} p_i^* (s_i - s_{i-1}) + \sum_{i=1}^{n} (t_i^* - t_{i-1}^*) H_i^*,$$

$$= \sum_{i=1}^{n} p_i^* (s_i - s_{i-1}) + \sum_{i=1}^{n} (t_i^* - t_{i-1}^*) H_i^*,$$

$$= \sum_{i=1}^{n} p_i^* (s_i - s_{i-1}) + \sum_{i=1}^{n} (t_i^* - t_{i-1}^*) H_i^*,$$

$$= \sum_{i=1}^{n} p_i^* (s_i - s_{i-1}) + \sum_{i=1}^{n} (t_i^* - t_{i-1}^*) H_i^*,$$

$$= \sum_{i=1}^{n} p_i^* (s_i - s_{i-1}) + \sum_{i=1}^{n} (t_i^* - t_{i-1}^*) H_i^*,$$

$$= \sum_{i=1}^{n} p_i^* (s_i - s_{i-1}) + \sum_{i=1}^{n} (t_i^* - t_{i-1}^*) H_i^*,$$

$$= \sum_{i=1}^{n} p_i^* (s_i - s_{i-1}) + \sum_{i=1}^{n} (t_i^* - t_{i-1}^*) H_i^*,$$

$$= \sum_{i=1}^{n} p_i^* (s_i - s_{i-1}) + \sum_{i=1}^{n} (t_i^* - t_{i-1}^*) H_i^*,$$

$$= \sum_{i=1}^{n} p_i^* (s_i - s_{i-1}) + \sum_{i=1}^{n} (t_i^* - t_{i-1}^*) H_i^*,$$

$$= \sum_{i=1}^{n} p_i^* (s_i - s_{i-1}) + \sum_{i=1}^{n} (t_i^* - t_{i-1}^*) H_i^*,$$

$$= \sum_{i=1}^{n} p_i^* (s_i - s_{i-1}) + \sum_{i=1}^{n} (t_i^* - t_{i-1}^*) H_i^*,$$

$$= \sum_{i=1}^{n} p_i^* (s_i - s_{i-1}) + \sum_{i=1}^{n} (t_i^* - t_{i-1}^*) H_i^*,$$

where

$$H_i^* \; \equiv \; \max_{d} \; \left\{ \rho_i^* U(d) - (1-\rho_i^*) L(d) - p_i^* d \right\} = \rho_i^* U(d_i^*) - (1-\rho_i^*) L(d_i^*) - p_i^* d_i^* .$$

is the (per-consumer) optimal surplus for tier i, cf. the Hamiltonian in (42). At the efficiency optimum, the resource shadow price μ equals the tier price p_i^* , by complementary slackness and market clearing; thus (51)–(52) express the standard identity "producer revenue + consumer surplus = social welfare."

V. CASE STUDIES AND REGIONAL COMPARISON

To verify the applicability and flexibility of the proposed variable-reliability market under different regional conditions, we examine two representative Chinese cities: Lanzhou in the northwest and Guangzhou on the southern coast. The former has abundant sunshine and relatively stable weather, representing a high-predictability PV environment; the latter is cloudier and rainier with stronger variability, representing a more challenging meteorological setting.

A. Parameter Settings and Output Modeling

According to national meteorological statistics, Lanzhou's average effective daylight duration is about 6.7 hours/day with a clear-sky share of roughly 65%, while Guangzhou's counterparts are 4.8 hours/day and 35%, respectively. Based on the diurnal baseline model in this paper, we simulate hourly PV output for a typical clear day in Lanzhou and a typical cloudy day in Guangzhou. We apply a weather attenuation factor $\eta(t)$ of 100% and 80%, respectively, and superimpose a cloud-induced disturbance term (author-specified for illustration rather than measured data). Minute-level series are used later to evaluate ramping cost. The resulting representative day profiles, $X_{\text{Lanzhou}}(t)$ and $X_{\text{Guangzhou}}(t)$, are shown in Fig. 9.

B. Availability G(x) Comparison

From the output sequences we compute the availability functions G(x) for both locations. As shown in Fig. 10, Lanzhou's availability dominates Guangzhou's across all thresholds, especially in the high-power region (e.g., x > 80 MW), where Lanzhou still has a significant chance of meeting the target while Guangzhou's probability is near zero. This indicates greater stability and reliability for Lanzhou's PV output.

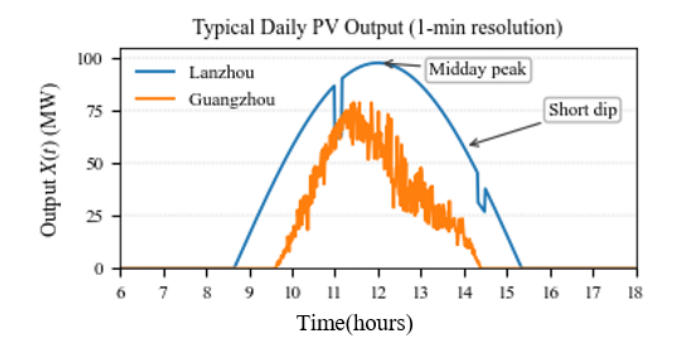


Fig. 9: Theoretical PV output profiles: Lanzhou (clear) vs. Guangzhou (cloudy).

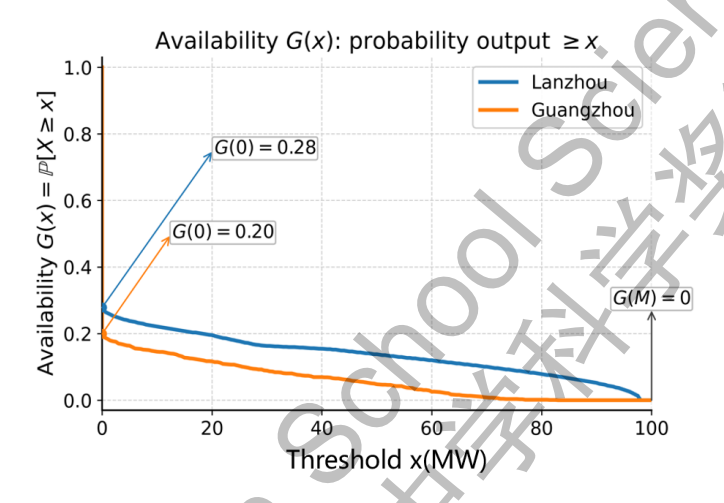


Fig. 10: Theoretical availability curves G(x): Lanzhou (clear) vs. Guangzhou (cloudy).

For illustration, a high-reliability contract at x=20 MW in Lanzhou achieves an empirical delivery rate close to 40%, aligned with its availability curve; a medium-reliability contract at the same x in Guangzhou delivers about 30%, reflecting higher meteorological uncertainty. The cross-regional differences in contract structures are direct mappings of the underlying availability curves and weather stability.

C. Ramping and Integration Cost Calculations

Using minute-level samples of the two representative-day profiles, we compute ramping cost via (5) in conjunction with figs. 9 and 10, and then evaluate the full-information and no-information integration costs via (11) and (16). The results are summarized in TABLE I.

TABLE I: Ramping and integration costs: Lanzhou vs. Guangzhou

Region	C _{ramp} (¥)	CI_1 (¥)	σ_1	CI_2 (¥)	σ_2
Lanzhou	62.68	651.97	23.71%	1125.18	40.92%
Guangzhou	1426.58	2015.87	73.30%	2489.08	90.51%

D. Contract Design

We now present a tiered contract design based on variable reliability. The core idea is to map the PV availability G(x) and discrete output states $\{s_j, \pi_j\}$ into a set of reliability tiers $\{\rho_k\}$, partition consumers by reliability preference, and then determine each tier's capacity d_k and price factor α_k .

a) Step 1: Determine reliability tiers ρ_k .: Discretize intra-day output into n states

$$0 < s_1 < s_2 < \dots < s_n, \qquad \sum_{j=1}^n \pi_j = 1.$$

Select $K \leq n$ tiers ordered by reliability. Define

$$\rho_k = \mathbb{P}[S \ge s_k] = \sum_{j=k}^n \pi_j, \qquad k = 1, \dots, K.$$
(53)

Alternatively, choose output thresholds x_k on G(x) and set $\rho_k = G(x_k)$.

b) Step 2: Partition consumers by preference.: Split $t \in [0,1]$ into K groups:

$$0 = t_0 < t_1 < \dots < t_K = 1,$$

where (t_{k-1},t_k) is the set of consumers choosing tier k, with share

$$\theta_k = t_k - t_{k-1}, \qquad \sum_{k=1}^K \theta_k = 1$$

c) Step 3: Determine tier capacities d_k : In state s_i , only contracts with reliability at least ρ_i are served. The supply constraint

$$\int_0^1 d(t) R_{\omega}(t) dt \le S(\omega)$$

implies a monotone allocation. For any i,

$$s_i = \sum_{j=1}^{i} d_j (t_j - t_{j-1}), \tag{54}$$

hence

$$s_i - s_{i-1} = d_i(t_i - t_{i-1}), \qquad d_i = \frac{s_i - s_{i-1}}{t_i - t_{i-1}}.$$
 (55)

- d) Step 4: Pricing (two common approaches).:
- 1) Cost-based: Given a base capacity price c_0 (¥/MW per period), introduce tier multipliers α_k :

$$p_k = \alpha_k c_0, \qquad \alpha_1 > \alpha_2 > \dots > \alpha_K.$$

Multipliers can reflect marginal social cost, reserve/ramping allocation, or calibrated coefficients.

2) Shadow-price: With shadow price μ for the reliability-filtered resource, a consumer's surplus

$$H(d, \rho, \mu) = \rho U(d) - (1 - \rho)L(d) - \mu d$$

implies at the optimum

$$\rho_k U'(d_k^*) - (1 - \rho_k) L'(d_k^*) = \mu = p_k,$$

so p_k increases with ρ_k .

For the Lanzhou/Guangzhou cases we use the first approach with $c_0=c$, i.e., $p_k=\alpha_k c$. One may set

$$\alpha_k = 1 + \gamma_1(\rho_k - \bar{\rho})$$

(linear or piecewise fits; γ_1 a tuning parameter).

e) Step 5: Tiered examples.: Using the computed G(x) and variability features, we list five illustrative tiers for each region: parameters $(\rho_k, \theta_k, d_k, \alpha_k)$ with prices $p_k = \alpha_k c$. See TABLE II (with M = 100 MW).

TABLE II: Illustrative tiered contracts: Lanzhou vs. Guangzhou

Region	Tier	$ ho_k$	θ_k	d_k (MW)	α_k	$p_k = \alpha_k c$
Lanzhou	1	0.95	15%	133.3	1.30	71.5
	2	0.80	35%	57.1	1.10	60.5
	3	0.50	30%	83.3	1.00	55.0
	4	0.15	15%	133.3	0.90	49.5
	5	0.00	5%	0.0	0.70	38.5
Guangzhou	1	0.95	5%	400.0	1.40	77.0
	2	0.80	15%	133.3	1.20	66.0
	3	0.50	25%	80.0	1.00	55.0
	4	0.20	35%	57.1	0.85	46.8
	5	0.00	20%	0.0	0.60	33.0

Here ρ_k is sampled from G(x), θ_k is an assigned consumer share, d_k follows (55), and α_k respects (1).

f) Discussion.: TABLE II reflects the regional differences in G(x) and cost structure. Lanzhou's availability is higher/flatter, allowing high-reliability tiers (e.g., $\rho \geq 0.8$) to cover a larger fraction of users with more balanced capacities. Guangzhou's high-power availability is much lower, so high-reliability products are scarce with larger markups, while mid/low tiers host more users and volume. Together with the previously computed C_{ramp} , CI_1 , CI_2 , and σ_1 , σ_2 , the results show that forcing PV into a single "firm" product would raise social subsidies—whereas the variable-reliability mechanism lets users with lower reliability needs voluntarily absorb quantity risk, reducing reserve requirements and balancing stress and improving price signals and total welfare. The case study demonstrates adaptation to different meteorology and regional features, achieving efficient allocation under heterogeneity.

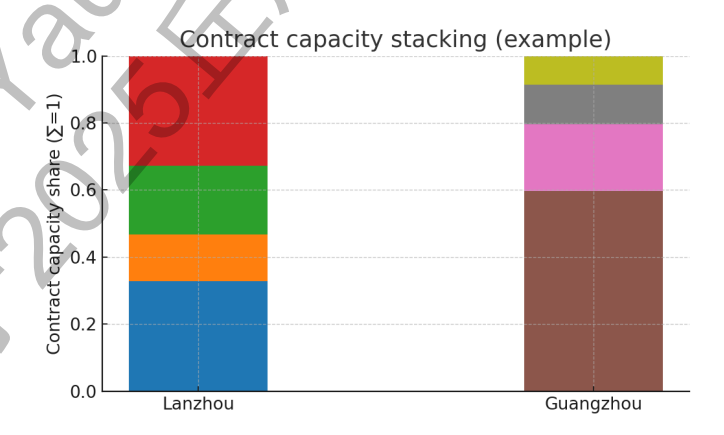


Fig. 11: Contract capacity stacking (example). Each bar shows the fraction of capacity allocated to reliability tiers $\{\rho_k\}$ in a region (normalized to $\sum_k = 1$). Colors follow the order in TABLE II (high to low ρ). Lanzhou exhibits a more balanced mix, consistent with a higher, flatter G(x); Guangzhou concentrates in mid/low tiers, indicating scarcity and higher markups for high-reliability products. This pattern aligns with regional differences in C_{ramp} , CI_1 , CI_2 , and σ_1 , σ_2 .

As shown in Fig. 11, we visualize the outcome by stacking the normalized contract capacities by reliability tier in each region. For region r, the height of tier k equals $\theta_k d_k / \sum_j \theta_j d_j$, so each bar sums to 1 and the composition—not the absolute level— is comparable across regions. Lanzhou exhibits a more balanced mix with substantial mass in high- ρ tiers, whereas Guangzhou concentrates in mid/low- ρ tiers and has only a thin high- ρ slice, reflecting the scarcity (and higher markups) of high-reliability products.

VI. CONCLUSION

Using minute resolution PV series, we first construct the availability curve G(x) and propose an indicator aggregation ramping metric that converts traditional \(\frac{1}{2}\)/MW·min charges into capacity commensurate \(\frac{1}{2}\)/MW, resolving the unit mismatch between regulation and capacity. We then derive closed form integration costs and subsidy rates under full, no, and partial information scenarios, quantifying the marginal value of forecast accuracy. Combining reliability stratification with a capacity price joint design, random output risk is endogenized within contracts, avoiding additional system wide reserves while maintaining real time balance. Finally, a Lanzhou (clear) vs. Guangzhou (cloudy) comparison illustrates regional adaptability: under highly variable minute scale conditions in Guangzhou, the social subsidy rate declines from about 90% under the traditional specification to below 70% with variable reliability, while Lanzhou remains around 25%. These results highlight the potential of variable reliability markets to reduce reserve needs, improve price signals, and enhance system economics for high penetration PV integration. Viewed through the lens of the green economy, our approach brings environmental and system variability externalities into contracts and settlement ex ante, delivering joint gains in efficiency and equity: dimensionally unified ramping metrics and availability profiling reduce reliance on rigid reserves and lower socialized integration costs, while reliability price menus and a priority rule align incentives via voluntary choice. This maps directly onto the UNEP emphasis on well being, equity, and lower environmental risk, and is consistent with the OECD/World Bank green growth focus on resource efficiency and resilience without sacrificing growth.

REFERENCES

- [1] California ISO, "Resource Adequacy," Generation & Transmission (web page). [Online]. Available: caiso.com
- [2] California ISO, Flexible Ramping Product: Technical Appendix, Jun. 10, 2015.
- [3] California ISO, Flexible Ramping Product Performance Report, Mar. 29, 2022.
- [4] California Public Utilities Commission (CPUC), "Resource Adequacy (RA) Program," (web page). [Online]. Available: cpuC.ca.gov
- [5] European Union, "Regulation (EU) 2019/943 on the internal market for electricity (recast)," Off. J., Jun. 5, 2019.
- [6] European Commission, "Capacity mechanisms," Energy (web page). [Online]. Available: energy.ec.europa.eu
- [7] SEM Committee (Ireland), I-SEM Capacity Remuneration Mechanism: Detailed Design Decision Paper, SEM-16-022, May 10, 2016.
- [8] Terna (Italy), "Capacity Market" (English portal). [Online]. Available: terna.it
- [9] Terna, Mercato della Capacità Disposizioni Tecniche di Funzionamento n. 1, 2024. (in Italian)
- [10] EnerNex Corporation, Eastern Wind Integration and Transmission Study, NREL Rep. SR-550-47078, 2010.
- [11] GE Energy, Western Wind and Solar Integration Study, NREL Rep. SR-550-47434, May 2010.
- [12] H. Holttinen et al., "Impacts of large amounts of wind power on the design and operation of power systems—results of IEA collaboration," in Proc. 8th Int. Workshop on Large-Scale Integration of Wind Power into Power Systems, Bremen, Germany, Oct. 2009.
- [13] North American Electric Reliability Corporation (NERC), Accommodating High Levels of Variable Generation, IVGTF Task 1.4, Aug. 2009.
- [14] State Grid Corporation of China (SGCC), Blue Book on Power System Flexibility Enhancement and New-type Power System Development, Beijing, China, 2022 (in Chinese).

- [15] W. Katzenstein and J. Apt, "The cost of wind power variability," Environmental Research Letters, vol. 7, no. 3, Art. 034019, 2012.
- [16] R. E. Bohn, M. C. Caramanis, and F. C. Schweppe, "Optimal spot pricing: Practices and theory," *IEEE Trans. Power Apparatus and Systems*, vol. PAS-101, no. 9, pp. 3234–3245, 1982.
- [17] R. E. Bohn, M. C. Caramanis, and F. C. Schweppe, "Optimal pricing in electrical networks over space and time," *RAND Journal of Economics*, vol. 15, no. 3, pp. 360–376, 1984.
- [18] H. P. Chao and R. B. Wilson, "Priority service: Pricing, investment, and market organization," *American Economic Review*, vol. 77, no. 5, pp. 899–916, 1987.
- [19] S. S. Oren, S. A. Smith, R. B. Wilson, and H. P. Chao, "Priority service: Unbundling the quality attributes of electric power," EPRI Interim Rep. EA-4851, Palo Alto, CA, 1986.
- [20] H. P. Chao, S. S. Oren, S. A. Smith, and R. B. Wilson, "Multilevel demand subscription pricing for electric power," *Energy Economics*, vol. 8, no. 4, pp. 199–217, 1986.
- [21] S. S. Oren and J. Doucet, "Interruption insurance for generation and distribution of electric power," *Journal of Regulatory Economics*, vol. 2, no. 1, pp. 5–19, 1990.
- [22] P. T. Ahlstrand, "Demand-side real-time pricing," in 1986 Annual Report, Pacific Gas & Electric Co., San Francisco, CA, 1987.
- [23] W. Vickrey, "Responsive pricing of public utility service," *Bell Journal of Economics and Management Science*, vol. 2, no. 1, pp. 337–346, 1971.
- [24] G. Brown and M. B. Johnson, "Public utility pricing and output under risk," *American Economic Review*, vol. 59, no. 1, pp. 119–128, 1969.
- [25] G. Brown and M. B. Johnson, "Welfare-maximizing price and output with stochastic demand: Reply," *American Economic Review*, vol. 63, no. 1, pp. 230–231, 1973.
- [26] M. Visscher, "Welfare-maximizing price and output with stochastic demand: Comment," *American Economic Review*, vol. 63, no. 1, pp. 224–229, 1973.
- [27] E. Bitar, R. Rajagopal, P. A. Kountouriotis, and P. Varaiya, "Designing markets for variable renewable energy," *IEEE Transactions on Power Systems*, vol. 37, no. 1, pp. 389–401, 2022.
- [28] E. Bitar, K. Poolla, P. P. Khargonekar, R. Rajagopal, P. Varaiya, and F. F. Wu, "Selling random wind," in *Proc. 45th Hawaii Int. Conf. on System Sciences (HICSS)*, Maui, HI, USA, 2012, pp. 1931–1937.
- [29] U. Helman, "Resource and transmission planning to achieve a 33% RPS in California—ISO modeling tools and planning framework," presented at the FERC Tech. Conf. on Planning Models and Software, Jun. 2010.
- [30] C. W. Tan and P. Varaiya, "Interruptible electric power service contracts," *Journal of Economic Dynamics and Control*, vol. 17, no. 3, pp. 495–517, 1993.
- [31] California Energy Commission, Renewable Portfolio Standard Annual Report, 2023.
- [32] Iberdrola Renewables, Bonneville Power Administration, and Constellation Energy, "Pilot project seeks to put more clean energy on the grid," *WindToday.net*, Sep. 22, 2010. [Online].
- [33] California ISO, Integration of Renewable Resources; Transmission and Operating Issues and Recommendations, 2007.
- [34] California ISO, Integration of Renewable Resources: Operational Requirements and Generation Fleet Capability at 20% RPS, 2010.
- [35] M. Del Franco, "Wind energy under fire within ERCOT," WindAction.org, Apr. 10, 2010. [Online].
- [36] C. W. Tan, Prices for Interruptible Electric Power Service, Ph.D. dissertation, Univ. of California, Berkeley, CA, 1990.
- [37] M. A. Crew and P. R. Kleindorfer, The Economics of Public Utility Regulation. Cambridge, MA, USA: MIT Press, 1986.
- [38] S. Kumar and R. Billinton, "Adequacy equivalents in composite power system evaluation," *IEEE Trans. Power Apparatus and Systems*, vol. PAS-87, no. 7, pp. 1167–1173, 1968.
- [39] G. Loury and T. Lewis, "On the profitability of interruptible supply," American Economic Review, vol. 76, no. 5, pp. 827-832, 1986.
- [40] M. G. Marchand, "Pricing power supplied on an interruptible basis," European Economic Review, vol. 5, no. 3, pp. 263-274, 1974.
- [41] C. K. Pang and A. J. Wood, "Multi-area generation system reliability calculations," *IEEE Trans. Power Apparatus and Systems*, vol. PAS-94, no. 3, pp. 508–517, 1975.
- [42] L. S. Pontryagin, V. G. Boltyanskii, R. V. Gamkrelidze, and E. F. Mishchenko, *The Mathematical Theory of Optimal Processes*. New York, NY, USA: Wiley, 1962.
- [43] R. Turvey, "Public utility pricing and output under risk: Comment," American Economic Review, vol. 60, no. 3, pp. 485-486, 1970.

致谢

盛行千里,不忘师恩。首先,感谢西安交通大学实验室的老师和学长、学姐,你们每次在我需要帮助的时候都给我极大的帮助。我要特别感谢我这篇论文的指导老师彭勤科教授。通过学校组织活动,认识了您,在假期课余时间进入实验室学习。作为我在经济建模领域的引路人,您不仅无偿为我提供了宝贵的学习机会和实践平台,更在学术上给予了我深入的指导和启发。从这篇设计的选题,撰写到制作完成,每一步都离不开彭勤科教授的悉心指导,您为我提供了许多宝贵的意见,正是因为您无私的帮助和鼓励,我才能顺利的完成论文,在此对您表示真诚的感谢。愿老师身体康健,桃李芬芳。

本研究从选题到最终成稿,始终在彭勤科教授的悉心指导下完成。老师负责宏观把握,提出了将光伏波动成本前移至合同层的研究思路,明确了以"可变可靠性市场设计"为核心的研究方向,并搭建了论文的整体框架。在老师确立的框架下,我具体开展了以下工作:进行文献检索,清洗和补全气象与功率数据,编写程序,完成三种信息情景下的成本推导与算例分析,设计分阶合同菜单,撰写论文初稿,并依据老师的反馈进行了多轮修改。研究过程中遇到的主要困难是"量纲统一"问题,老师在讨论中提出了关键的解决思路,我据此重新整理了公式体系、调整了算例设计并补充了相关分析,使该问题最终得以解决。衷心感谢彭老师在时间安排、计算资源以及投稿事宜上给予的全力支持,同时也感谢各位学长学姐在代码编写方面的耐心指导。